Metal-insulator transition in random Kronig-Penney superlattices with long-range correlated disorder

A. Esmailpour,[1,2] M. Esmaeilzadeh,[1] E. Faizabadi,[2] P. Carpena,[3] and M. Reza Rahimi Tabar[4,5]
[1]*Department of Physics, Iran University of Science and Technology, Narmak, Tehran 16844, Iran*
[2]*Department of Physics, Shahid Rajaei University, Lavizan, Tehran 16788, Iran*
[3]*Departmento de Física Aplicada II, ETSI de Telecomunicación, Universidad de Málaga, 29071 Málaga, Spain*
[4]*Department of Physics, Sharif University of Technology, Tehran 11365-9161, Iran*
[5]*CNRS UMR 6202, Observatoire de la Cote d'Azur, BP 4229, 06304 Nice Cedex 4, France*
(Received 15 March 2006; revised manuscript received 1 June 2006; published 25 July 2006)

We study the electronic properties of disordered GaAs-$Al_xGa_{1-x}As$ semiconductor superlattices with structural long-range correlations. The system consists of quantum barriers and wells with different thicknesses and heights which fluctuate around their mean values randomly, following a long-range correlated pattern of fractal type characterized by a power spectrum of the type $S(k) \propto 1/k^{(2\alpha-1)}$, where the exponent α quantifies the strength of the long-range correlations. For a given system size, we find a critical value of the exponent α (α_c) for which a metal-insulator transition appears: for $\alpha < \alpha_c$ all the states are localized, and for $\alpha > \alpha_c$, we find a continuous band of extended states. We also show that the existence of extended states causes a strong enhancement of the dc conductance of the superlattice at finite temperature, which increases in many orders of magnitude when crossing from the localized to the extended regime. Finally, we perform finite size scaling and we obtain the value of the critical exponent α_c in the thermodynamic limit, showing that the transition is not a finite-size effect.

DOI: 10.1103/PhysRevB.74.024206 PACS number(s): 71.23.An, 71.30.+h, 72.15.Rn

I. INTRODUCTION

It is known that all electron states in disordered one- and two-dimensional systems are exponentially localized for any amount of uncorrelated disorder.[1] In recent years, a number of tight-binding[2–4] and continuous[5] models have predicted the existence of extended states for disordered one-dimensional (1D) systems with *short-range* correlation. It is shown that GaAs-$Al_xGa_{1-x}As$ semiconductor superlattices (SSLs) with random dimmer wells exhibit high dc conductance.[5–7] Experimental evidence of the delocalization effect produced by these short-range correlations was recently found in semiconductor superlattices.[8] Also recently, the interest for 1D disordered models with correlated disorder has been growing, as it has become progressively clear that correlations of the random potential can deeply affect the electronic localization properties, since spatial correlations of the disorder can unexpectedly create extended states at some particular energies. The effects of long-range correlated disorder in the electronic properties of 1D solids was first studied in Ref. 9 and 10, where a metal-insulator transition driven by the degree of correlations was reported. Later work confirms this result and/or extends it to other models,[11–14] and a simple physical picture of the transition can be seen in Ref. 15. Long-range correlations also affect the level statistics of the system, which can also experience a transition from a Poissonian to a non-Poissonian phase.[16] Recent works have studied the delocalization effects produced when nonrandom long-range intersite coupling are considered[17] and when long-range correlations are introduced in the hopping terms of the Hamiltonian.[18] To understand the effect of long-range correlations of the disorder on a phase transition, Izrailev *et al.* perturbatively derived an analytical relationship between localization length and potential pair correlators.[19] They showed how specific long-range disorder correlations lead to the appearance of mobility edges in 1D discrete systems. An experimental confirmation of these findings was obtained by studying the transmission of microwaves in a single-mode waveguide with a random array of correlated scatterers.[20]

In this paper, our aim is to study the electronic behavior of GaAs-$Al_xGa_{1-x}As$ SSLs with structural long-range correlations by means of the transfer matrix method. The SSLs, which are modeled according to a Kronig-Penney structure, consist of GaAs quantum wells and $Al_xGa_{1-x}As$ barriers. We consider three different ways to introduce long-range correlated disorder in the SSL: (i) the width of the wells fluctuates around its mean value, (ii) the width of the barriers fluctuate also around their mean values and finally, (iii) height fluctuations of the barriers. For the mentioned three cases, we study the effect of the long-range correlations in the localization length and in the dc conductance for SSLs of finite size, showing the existence of a metal-insulator transition driven by the correlations. We are also able to calculate the behavior of the system in the thermodynamic limit, to prove that the transition is not simply a finite-size effect. Although the metal-insulator transition driven by long-range correlation has been previously reported,[9–14] in all these cases a tight-binding approach was considered. Here we show that this type of transition also occurs using other models (Kronig-Penney-like), which enriches the phenomenon. In addition, as the superlattice model considered here is more adequate to describe real superlattices, our results can be useful for possible technological applications, since depending on the strength of the correlations introduced in a superlattice, its electronic properties can be modified at will.

This paper is organized as follows: in Sec. II we focus on the details of the model and we derive the related transfer

matrix. We also explain how we calculate the localization length and dc conductance, and how we generate the long-range correlated-disordered series. In Sec. III we present and discuss our numerical results. Finally, Sec. IV ends the paper with a summary of our results.

II. MODEL AND METHOD

A. Superlattice model

We consider a GaAs-$Al_xGa_{1-x}As$ semiconductor superlattice structure under the envelope function approximation, i.e., represented as a Kronig-Penney model. A single quantum well (QW) in this structure consists of a layer with thickness d_W of a semiconductor A (GaAs) embedded in a semiconductor B ($Al_xGa_{1-x}As$). The thickness of layer B is assumed to be d_b. We consider the situation in which the values of d_W and d_b (also the height of the barriers, which is explained below) fluctuate around their mean values, a and b. The fluctuations are given by $d_w^n = a(1+\delta\epsilon_n)$ and $d_b^n = b(1+\delta\epsilon_n)$, respectively. Here $\{\epsilon_n\}$ is a set of random variables with long-range correlations which are characterized by a spectral density $S(k) \propto 1/k^{(2\alpha-1)}$, and the way in which we generate it is explained in Sec. II B. The exponent α quantifies the strength of the correlations, δ is a positive parameter measuring the maximum deviation from the mean value, and n is the site index (in this case, the barrier number).

The SSL potential derives directly from the different energies of the conduction and valence band edges at the interfaces. In the simplest picture, the SSL potential is:

$$V_{SSL} = \begin{cases} \Delta E_C^n, & \text{if } |x - x_n| < \dfrac{d_b^n}{2}; \\ 0, & \text{otherwise,} \end{cases} \tag{1}$$

where ΔE_c^n is the conduction-band offset defined as $E_{CB}^n - E_{CA}^n$ and x_n denotes the position of the center of the nth barrier. The energy is measured from the bottom of the conduction band in the semiconductor A (i.e., $E_{CA}^n = 0$). We consider the electronic states with energy below the barrier energy ($E < \Delta E_C^n$), which are the most interesting ones to study quantum confinement effects. When considering that the correlated disorder affects the barrier height, we use $\Delta E_C^n = \Delta E_C(1+\delta\epsilon_n)$, where ΔE_C is the average value of the barrier height ($\Delta E_C = 0.25$ eV in all the calculations). Using the one-band effective-mass frame the Schrödinger equation for the electron wave functions can be written as follows:

$$\left[-\frac{\hbar^2}{2m}\frac{d^2}{dx^2} + V_{SSL}(x) \right] \psi(x) = E\psi(x), \tag{2}$$

where an explicit dependence of both E and $\psi(x)$ on quantum numbers is omitted and x is the direction perpendicular to the SSL layers. We have taken constant effective mass at the Γ valley. The envelope function in the QW between the barriers centered at x_n and x_{n+1} is:

$$\psi_W^n(x) = p_W^n \exp\left(ik_W\left(x - x_n - \frac{d_b^n}{2} \right) \right) + q_W^n \exp\left(-ik_W\left(x - x_n - \frac{d_b^n}{2} \right) \right) \tag{3}$$

for $x_n + \frac{d_b^n}{2} < x < x_{n+1} - \frac{d_b^n}{2}$ and p_W^n, q_W^n are two constants to be determined later. The wave number is given by $k_W^2 = \frac{2m_W E}{\hbar^2}$, where m_W is the effective mass in the quantum wells. Inside the nth barrier the envelope function is:

$$\psi_b^n(x) = p_b^n \exp(-k_b x) + q_b^n \exp(k_b x) \tag{4}$$

for $x_n - \frac{d_b^n}{2} < x < x_n + \frac{d_b^n}{2}$ and $k_{b,n}^2 = \frac{2m_b(\Delta E_c^n - E)}{\hbar^2}$, where m_b is the effective mass in the quantum barriers. The coefficients p_b^n and q_b^n are determined by using boundary conditions. Imposing continuity of $\psi(x)$ and $\frac{1}{m}\frac{d\psi(x)}{dx}$ at the interfaces, the envelope-function values at both sides of the nth barrier are related by using the conventional transfer matrix method of the form:

$$\begin{pmatrix} p_W^n \\ q_W^n \end{pmatrix} = \begin{pmatrix} \alpha_n & \beta_n \\ \beta_n^* & \alpha_n^* \end{pmatrix} \begin{pmatrix} p_W^{n-1} \\ q_W^{n-1} \end{pmatrix}, \tag{5}$$

where α_n and β_n are defined as follows:

$$\alpha_n = \left[\cosh(k_{b,n} d_b^n) + \frac{i}{2}\left(\frac{m_b k_W}{m_W k_{b,n}} - \frac{m_W k_{b,n}}{m_b k_W} \right) \sinh(k_{b,n} d_b^n) \right] \times \exp(ik_W d_W^n)$$

$$\beta_n = -\frac{i}{2}\left(\frac{m_b k_W}{m_W k_{b,n}} + \frac{m_W k_{b,n}}{m_b k_W} \right) \sinh(k_{b,n} d_b^n) \exp(-ik_W d_W^n). \tag{6}$$

The wave function of the SSL ends can be related together by calculating a product of transfer matrices as $P_{N,1} = \Pi_{n=1}^N P_{n,n-1}$. In this equation N is the number of barriers and $P_{n,n-1}$ is the transfer matrix which connects the wave functions of sites n and $n-1$. According to the component of this matrix, the Lyapunov exponent is (Ref. 21)

$$\tilde{\gamma} = \frac{1}{L} \ln \frac{\|P_{L,1}\nu_0\|}{\|\nu_0\|}, \tag{7}$$

where ν_0 is the starting vector and L indicates the total length of the system which in our model $L = N(<d_W^n> + b)$ or $L = N(<d_b^n> + a)$ for fluctuating d_W^n or d_b^n, respectively. The matrix $P_{L,1}$ is calculated iteratively and the Lyapunov exponent γ is evaluated using Eq. (7). The Lyapunov exponent is a suitable variable to describe localization properties, because it is related to the exponential decreasing of the wave function. An important property of the Lyapunov exponent is that it satisfies a multiplicative central limit theorem[22] and approaches a nonrandom limit γ when the size of the system L tends to infinity. The localization length λ of a state with a given energy E in the infinite system is related to γ as $\lambda = \gamma^{-1}$. At finite system size L, it is a random quantity with a mean value equal to the infinite limit (i.e., $\langle\tilde{\gamma}\rangle = \gamma$). The knowledge of the Lyapunov exponent γ enables us to obtain

the transmission coefficient at a given energy by using $\tau=\exp(-L\gamma)$. The dimensionless finite-temperature dc conductance is computed by using the following expression that was discussed in detail by Engquist and Anderson (Ref. 23).

$$k(\mu,T)=\frac{\int\left(-\frac{\partial f}{\partial E}\right)\tau(E)dE}{\int\left(-\frac{\partial f}{\partial E}\right)[1-\tau(E)]dE}. \quad (8)$$

Here f is the Fermi-Dirac distribution and μ denotes the chemical potential of the system.

B. Generating correlations

We would like study metal-insulator transition in disordered GaAs-$Al_xGa_{1-x}As$ semiconductor superlattices with structural long-range correlations. Thus, we first need to generate long-range correlated sequences of random variables. A sequence of long-range correlated values $\{\varepsilon_i\}$ is produced by the Fourier filtering method in the Makse *et al.* version.[24] This method is based on a transformation of the Fourier components $\{u_k\}$ of a random number sequence $\{u_i\}$ which are uncorrelated random numbers following a Gaussian distribution. A sequence of $\{\varepsilon_k\}$ is generated for a given α using the formula: $\varepsilon_k=k^{-(2\alpha-1)/2}u_k$. Inverse Fourier transformation of the sequence $\{\varepsilon_k\}$ leads to the sequence of interest $\{\varepsilon_i\}$. The resulting sequence of random variables are spatially correlated with spectral density

$$S(k)\propto k^{-(2\alpha-1)}, \quad (9)$$

and they have Gaussian distribution. The exponent α is called the correlation exponent, and quantifies the degree of correlations imposed in the system. With the definition in (9) α corresponds to the exponent provided by detrended fluctuation analysis (DFA), which is one of the most widely used methods to quantify long-range correlations.[26–28] Note that the case $\alpha=0.5$ corresponds to uncorrelated disorder (white noise), while the case $\alpha>0.5$ indicates positive correlations. Several examples of correlated sequences for different values of the correlation exponent α are shown in Fig. 1. We note that the sequences produced by this method are normalized, so that the mean value $\langle\varepsilon_i\rangle$ is set to zero and its variance is fixed to unity.

Note that using this method, it is not possible to introduce spurious periodicities in the final series, since a power-law power spectrum is granted, and also because the starting point is a fully random sequence produced by a random number generator. Therefore, unless the random generator presents a very small period (smaller than the generated sequences) spurious periodicities cannot appear. As we employ widely used and well-tested random number generators[25] with periods many orders of magnitude larger than the sequences we consider in this paper, we are confident that such periodicities do not appear.

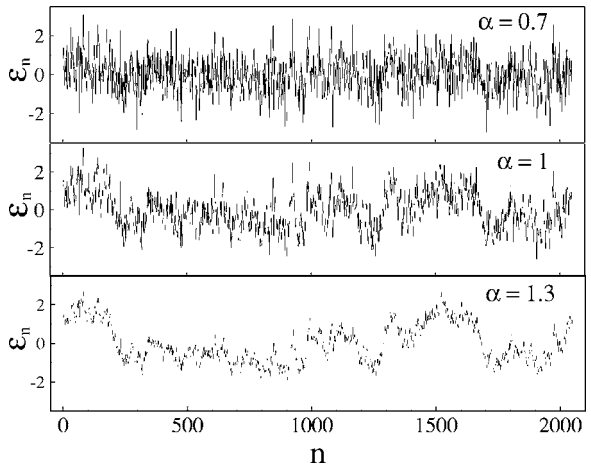

FIG. 1. Three examples of series of long-range correlated random values generated with the Fourier filtering method for different values of the correlation exponent α.

III. NUMERICAL RESULTS

A. Localization length

Using the methods described above, here we calculate the Lyapunov exponent and study the localization length of long-range correlated-disordered SSLs as a function of the strength of the correlations introduced in the system (the exponent α). The energy is assumed to be less than the barrier heights ($E<\Delta E_C^n$).

In all the calculations carried out in this section, the common structural factors are assumed to be $a=25$ Å, $b=25$ Å, $x=0.35$, $m_W=0.067\,m$, and $m_b=0.096\,m$, which corresponds to a GaAs-$Al_xGa1_{1-x}As$ SSL, where x indicates the Al mole fraction at the barriers, and m is the electron mass.

In all the cases we consider below, we calculate the localization length λ as a function of energy E for the finite system size L for different values of the correlations imposed in the system. When the localization length starts to be greater than the system size ($\lambda\geqslant L$), we say that a transition from localized states (insulator) to extended states (metal) is observed *for the finite system size*. The α value at which the transition is detected for a fixed L is called $\alpha_c(L)$. We also want to point out that in the numerical results we present below in Figs. 2–4, we only show results for α values close to the corresponding α_c, i.e., for disordered systems with strong long-range correlations (high α values). In general, for disordered systems without correlations (corresponding to $\alpha=0.5$) the electronic states are strongly localized, and the localization length is very small (much smaller than the cases shown in Figs. 2–4).

Figure 2 shows the localization length as a function of energy for different values of the correlation exponent α when the thickness of the wells fluctuates around the mean value a in the form $d_W^n=a(1+\delta\epsilon_n)$. The other structural parameters we have used in the calculation are $\delta=0.1$, $d_b^n=25$ Å, and $\Delta E_C^n=0.25$ eV. Note that these parameters correspond to keep fixed the barrier height and width. As shown in Fig. 2, in all the cases considered the localization length presents a maximum value around $E=0.15$ eV. However, for

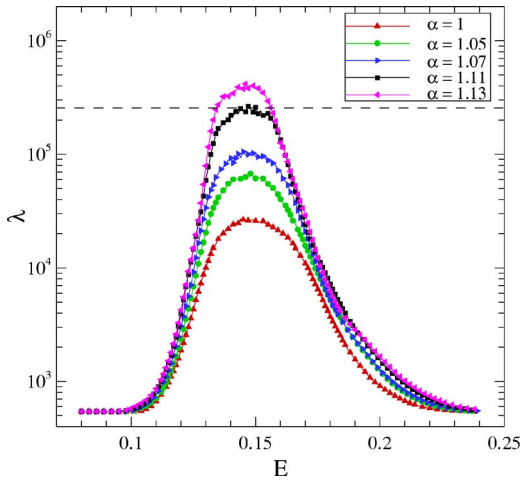

FIG. 2. (Color online) Plot of the localization length in the SSL as a function of the energy for different values of the correlation exponent α for the case in which the thickness of wells fluctuates around its mean value and the width and height of the barriers are kept constant. The dashed line indicates the system size $L=250\,000$.

low correlations (low α), the localization length λ is smaller than the system size L in the whole energy range, and therefore all the states are localized, as expected in a disordered system. When increasing correlations, we observe how in general the localization length also increases, and eventually at $\alpha \simeq 1.11$ the localization length starts to be larger than the systems size L in the central region of energy. For $\alpha \geqslant 1.11$, this effect is more pronounced, and there exists a continuum of extended states for which $\lambda > L$. In this sense, for the case shown in Fig. 2, we say that the value at which the localization-delocalization transition occurs is $\alpha_c = 1.11$. Note that this transition is shown in a system with *finite* size, but

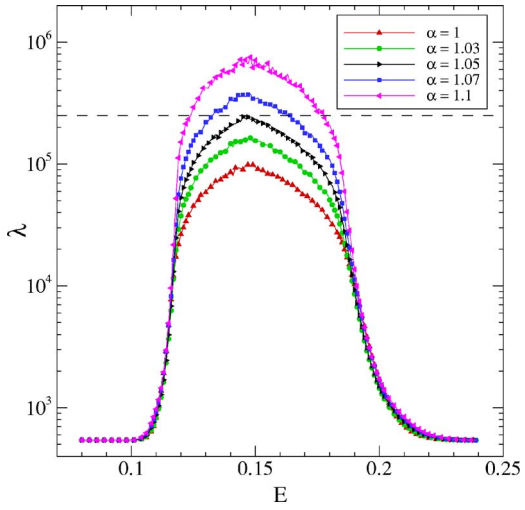

FIG. 3. (Color online) Plot of the localization length in the SSL as a function of the energy for different values of the correlation exponent α for the case in which the width of the barriers fluctuate around its mean value and the thickness of wells and the height of barriers are kept constant. The dashed line indicates the system size $L=250\,000$.

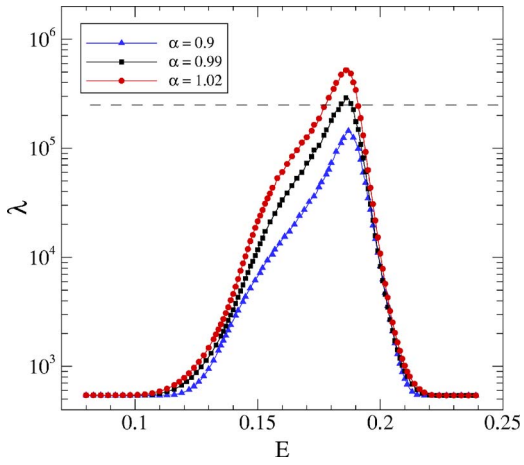

FIG. 4. (Color online) Plot of the localization length in the SSL as a function of the energy for different values of correlation exponent α when the height of the barriers fluctuate around its mean value and the thickness the of wells and the width of the barriers are kept constant. The dashed line indicates the system size $L=250\,000$.

below we will discuss the situation in the thermodynamic limit.

Now, we study the case in which the thickness of the wells d_W^n and height of the barriers ΔE_C^n are kept fixed, while the width of the barriers fluctuates around the mean value in the form $d_b^n = b(1+\delta\epsilon_n)$. Our numerical results are shown in Fig. 3 where we plot the localization length as a function of energy for different values of correlation exponent α. The numerical values of the structural parameters used are $\delta=0.1$, $d_W^n=25$ Å, and $\Delta E_C^n=0.25$ eV, respectively. We see how the behavior of λ as a function of energy is qualitatively similar in the present case (correlated disorder in the width of the barriers) than in the case shown in Fig. 2 (correlated disorder in the thickness of the wells). For a fixed system size L, the localization length presents also in general a maximum around $E=0.15$ eV. For low correlations, all the electronic states are localized ($\lambda < L$), while by increasing α the localization length λ increases in the whole energy range. In this case, for the numerical values considered, we observe the localized-extended transition at $\alpha_c = 1.05$. For larger values of α we observe again a continuum of extended states for which $\lambda > L$. Note that this transition is observed for a finite system size, while the thermodynamic limit is discussed later.

Finally, we want to study the behavior of the electronic localization length λ when the height of the barriers ΔE_C^n fluctuates around the mean value ΔE_C in the form $\Delta E_C^n = \Delta E_C(1+\delta\epsilon_n)$, while we keep fixed the thickness of the wells and the width of the barriers. Figure 4 shows the localization length λ as a function of energy for several values of the correlation exponent α for a SSL with the following structural parameters: $\delta=0.17$, $\Delta E_C=0.25$ eV, $d_b^n=25$ Å, and $d_w^n=25$ Å. As in the two previous cases, we observe that λ presents a maximum (now around $E \simeq 0.18$ eV). For low values of the correlation exponent α, all the electronic states are localized. When increasing correlations, the localization length increases in the whole energy range, and now ex-

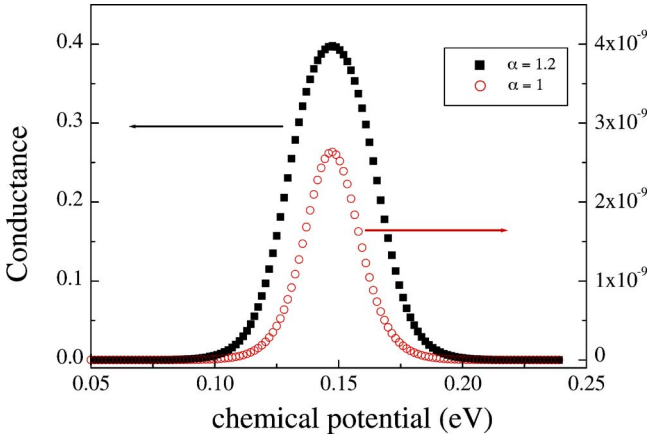

FIG. 5. (Color online) Graph of the dc conductance as a function of chemical potential at 77 K for two values of correlation exponent (α=1,1.2). The other parameters are the same as in Fig. 2. Note that the scale of the diagram for α=1 is at the right-hand side of the figure, while for α=1.2 is at the left-hand side of the figure.

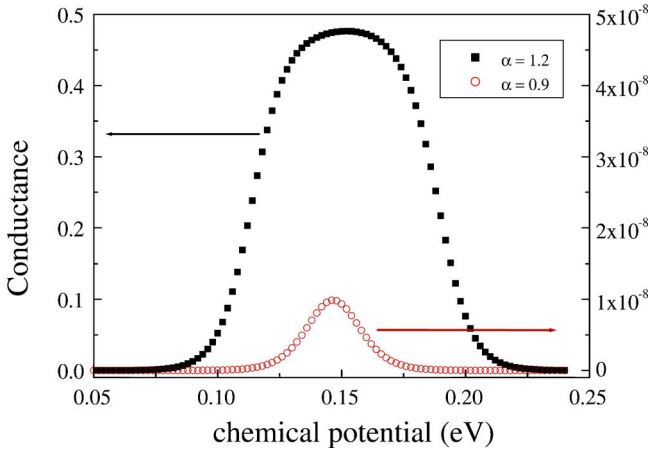

FIG. 6. (Color online) Graph of the dc conductance as a function of chemical potential at 77 K for two values of correlation exponent (α=0.9,1.2). The other parameters are the same as in Fig. 3. Note that the scale of the diagram for α=0.9 is at the right-hand side of the figure, while for α=1.2 is at the left-hand side of the figure.

tended states for which $\lambda > L$ start to appear at α_c=0.99. For the case $\alpha > \alpha_c$, a continuum of extended states would appear in a band centered at $E \simeq 0.18$ eV, as we show in Fig. 4.

Although the numerical details of the three cases shown in Figs. 2–4 are different, the general behavior is common: in all cases there exists a critical value of the correlations introduced in the disordered system above which there is a continuous band of extended states. Thus, long-range correlations are able to change the expected behavior in a disordered superlattice, where all the states are localized for *uncorrelated* disorder. Note that this behavior has been shown for finite system size, but a real metal-insulator transition only happens in the thermodynamic limit, which is discussed below.

B. dc conductance

In this section we study if the delocalization effect introduced by the correlations in the disordered SSL is also reflected in the conducting properties of the superlattice. Thus, we have calculated numerically the electrical dc conductance as a function of the chemical potential using Eq. (8), considering a different degree of correlations imposed in the system, just below and above the corresponding α_{cr}.

Our results for two different correlation exponents α are shown in Figs. 5 and 6, where a temperature of 77 K has been considered. Figure 5 corresponds to the case in which the correlated disorder is present in the thickness of the wells, and the other structural parameters are the same as the ones in Fig. 2. Figure 5 corresponds to the case in which the correlated disorder is present in the width of the barriers, and the other parameters are identical as the ones in Fig. 2. Both cases present qualitatively identical behavior, which can be summarized in two main ideas: (i) the conductance of the system presents a maximum when the chemical potential equals the energies for which the localization length reaches the maximum values, as expected, resembling Figs. 5 and 6 very well the results shown in Figs. 2 and 3, respectively. And (ii), more relevant for our study, correlations very much enhance the conductance of the SSL, and this enhancement is dramatic when the correlations imposed in the system are larger than the corresponding α_c. For example, in the cases shown in Figs. 5 and 6, we plot the results for two values of α, one below and the other one above the corresponding critical values (1.11 and 1.05 for Figs. 5 and 6, respectively). We observe that when $\alpha > \alpha_c$, the conductance increases in about eight orders of magnitude when compared to the case $\alpha < \alpha_c$. This effect supports the existence of a metal-insulator transition driven by the long-range correlations imposed in the SSL.

Note that we have shown the existence of a metal-insulator transition using the behavior of the localization length, and also of the conductance. But in both cases we have considered a system with large but finite size (we have used L=250 000 in all the calculations). The remaining question is then if this transition is a mere finite size effect, or if it can be also detected in the thermodynamic limit. This is discussed in Sec. III C.

C. Thermodynamic limit

We have discussed above that there exists a critical value of the correlations imposed in the SSL α_c, defined as the values of the correlation at which extended states start to appear, i.e., the minimum α value needed to have the localization length λ larger or equal to the system size L. In all the results shown before, we have considered a large but fixed system size (L=250 000), but clearly the critical correlation exponent α_c is not independent of the system size L, so actually we should write $\alpha_c(L)$. Precisely the behavior of $\alpha_c(L)$ as a function of L can tell us if the transition we have reported above is a finite-size effect or if it also appears in the thermodynamic limit, becoming a real phase transition. Thus, we have studied systematically the behavior of α_c as a func-

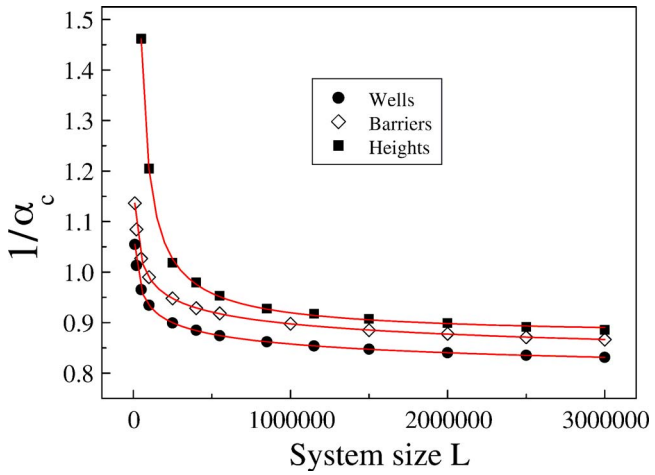

FIG. 7. (Color online) The inverse of the critical correlation exponent $\frac{1}{\alpha_c}$ as a function of the system size L (symbols). The cases shown are calculated with the same parameters as in Figs. 2–4. The solid lines correspond to fits according to model (10).

tion of L, and the results are shown in Fig. 7, where we plot for convenience $1/\alpha_c$ as a function of L for a wide range of system sizes (up to $L=3\times10^6$) and for the three cases considered in Sec. III A: correlated disorder in the well thickness, in the barrier width, and in the barrier heights. We want to stress that in the Kronig-Penney model used in all our calculations we do not consider the effect of roughness at the interfaces (which surely would modify the thermodynamic limit studied in this section), since we want to show the transition in the simplest possible superlattice model.

A real transition exists if α_c remains finite in the thermodynamic limit $L\to\infty$. To show that this is precisely our case, we fit the data shown in Fig. 7 using a model of the type:

$$\frac{1}{\alpha_c} = z + \frac{r}{L^{\eta}}, \tag{10}$$

where z, r, and η are constants to be determined in the fitting procedure. It is clear that z^{-1} is the asymptotic value of α_c at the thermodynamic limit $L\to\infty$, which we call $\alpha_c(\infty)$. The model (10) produces excellent fittings in the numerical data shown with symbols in Fig. 7. The fittings are represented in solid lines in Fig. 7, and in all cases we find that $r^2>0.999$. Following this procedure, we obtain $z=0.72$, $z=0.74$, and $z=0.87$, for correlated disorder in the thickness of the wells, the width of the barriers, and the height of the barriers, respectively. Using that $\alpha_c(\infty)=z^{-1}$, we find that the critical correlation exponents in the thermodynamic limit are $\alpha_c(\infty)=1.39$, $\alpha_c(\infty)=1.36$, and $\alpha_c(\infty)=1.15$ for correlated disorder in the thickness of the wells, the width of the barriers, and the height of the barriers, respectively. Thus, we are reporting a real metal-insulator transition and not a finite-size effect. We want to point out that the particular values of $\alpha_c(\infty)$ we have determined in the three cases shown in Fig. 7 depend on the value of the parameter δ considered, which essentially measures the variance of the correlated disordered series of the corresponding structural parameter. Thus, by choosing different δ values, different $\alpha_c(\infty)$ are expected, but the existence of the transition, which is our main result, is independent of the particular δ value. These results are in contrast with the single critical value $\alpha_c(\infty)=1.5$ corresponding to a tight-binding model first found in (Ref. 9) and confirmed by later work. This seems to indicate that in correlated-disordered Kronig-Penney superlattices, and considering that the disorder enters only in one structural parameter, there is not a single critical value of the correlations $\alpha_c(\infty)$ at which the metal-insulator transition occurs, but a critical (hyper)surface controlled by the multiplicity of parameters involved in the model (wells and barriers parameters and variance δ of the correlated-disordered magnitude). Therefore, there will be an $\alpha_c(\infty)$ value for any value of δ and any combination of structural parameters, so that the determination of the complete phase diagram is of great difficulty and out of the scope of the present study.

IV. CONCLUSION

We study the electronic properties of quantum well-based long-range correlated random superlattices by calculating numerically the localization length and dc conductance for different degrees of correlations imposed in the system. For any finite system size, it is shown that there exists a critical value in the correlations imposed in the system below which all the electronic states are localized and above which we find a band of finite width of extended states. This critical value of the correlations at which the localization-delocalization transition occurs depends on the structural parameter in which the correlated disorder is introduced (well thickness, barrier width or barrier height), and also on the strength of the disorder. In addition we demonstrate that these delocalized states reveal themselves through a dramatic enhancement of the dc conductance at finite temperature, which increases in many orders of magnitude when the correlation in the system is larger than the critical value. In addition, by performing finite-size scaling, we find that the transition is not a finite size effect, because we calculate the critical correlation exponent at the thermodynamic limit $\alpha_c(\infty)$.

ACKNOWLEDGMENTS

P.C. acknowledges financial support from the Spanish Government (Grants Nos. BFM2002-00183 and BIO2005-09116-C03-01).

[1] P. W. Anderson, Phys. Rev. **109**, 1492 (1958).
[2] D. H. Dunlap, H. L. Wu, and P. W. Phillips, Phys. Rev. Lett. **65**, 88 (1990).
[3] P. Philips and H. L. Wu, Science **252**, 1805 (1991).
[4] J. C. Flores, J. Phys.: Condens. Matter **1**, 8479 (1989).
[5] E. Diez, A. Sánchez, and F. Domínguez-Adame, Phys. Rev. B **50**, 14359 (1994).
[6] F. Domínguez-Adame, A. Sánchez, and E. Diez, Phys. Rev. B **50**, 17736 (1994).
[7] E. Diez, A. Sánchez, and F. Domínguez-Adame, IEEE J. Quantum Electron. **31**, 1919 (1995).
[8] V. Bellani, E. Diez, R. Hey, L. Toni, L. Tarricone, G. B. Parravicini, F. Domínguez-Adame, and R. Gomez-Alcala, Phys. Rev. Lett. **82**, 2159 (1999).
[9] F. A. B. F. de Moura and M. L. Lyra, Phys. Rev. Lett. **81**, 3735 (1998).
[10] F. A. B. F. de Moura and M. L. Lyra, Physica A **266**, 465 (1999).
[11] P. Carpena, P. Bernaola-Galván, P. Ch. Ivanov, and H. E. Stanley, Nature (London) **418**, 955 (2002).
[12] F. A. B. F. de Moura, M. D. Coutinho-Filho, E. P. Raposo, and M. L. Lyra, Phys. Rev. B **66**, 014418 (2002); **68**, 012202 (2003).
[13] F. Dominguez-Adame, V. A. Malyshev, F. A. B. F. de Moura, and M. L. Lyra, Phys. Rev. Lett. **91**, 197402 (2003).
[14] H. Shima, T. Nomura, and T. Nakayama, Phys. Rev. B **70**, 075116 (2004).
[15] E. Diaz, A. Rodriguez, F. Dominguez-Adame, and V. A. Malyshev, Europhys. Lett. **72**, 1018 (2005).
[16] P. Carpena, P. Bernaola-Galván, and P. Ch. Ivanov, Phys. Rev. Lett. **93**, 176804 (2004).
[17] F. A. B. F. de Moura, A. V. Malyshev, M. L. Lyra, V. A. Malyshev, and F. Domínguez-Adame, Phys. Rev. B **71**, 174203 (2005).
[18] F. Shahbazi, A. Bahraminasab, S. Mehdi Vaez Allaei, M. Sahimi, and M. R. Tabar, Phys. Rev. Lett. **94**, 165505 (2005).
[19] F. M. Izrailev and A. A. Krokhin, Phys. Rev. Lett. **82**, 4062 (1999).
[20] U. Kuhl, F. M. Izrailev, A. A. Krokhin, and H.-J. Stockmann, Appl. Phys. Lett. **77**, 633 (2000).
[21] L. I. Deych, M. V. Erementchouk, A. A. Lisyansky, A. Yamilov, and H. Cao, Phys. Rev. B **68**, 174203 (2003).
[22] V. I. Oseledets, Trudy Moskov. Mat. Obshch. **47**, 179 (1968).
[23] H. L. Engquist and P. W. Anderson, Phys. Rev. B **24**, 1151 (1981).
[24] H. A. Makse, S. Havlin, M. Schwart, and H. E. Stanley, Phys. Rev. E **53**, 5445 (1996).
[25] W. H. Press *et al.*, *Numerical Recipes in Fortran: the Art of Scientific Computing* (Cambridge University Press, Cambridge 1989).
[26] K. Hu, P. C. Ivanov, Z. Chen, P. Carpena, and H. E. Stanley, Phys. Rev. E **64**, 011114 (2001).
[27] Z. Chen, K. Hu, P. Carpena, P. Bernaola-Galván, H. E. Stanley, and P. C. Ivanov, Phys. Rev. E **71**, 011104 (2005).
[28] A. V. Coronado and P. Carpena, J. Biol. Phys. **31**, 121 (2005).